Synthesis and solution properties of a temperature-responsive PNIPAM–b-PDMS–b-PNIPAM triblock copolymer

Article

Accepted Version

Synthesis and solution properties of a temperature-responsive PNIPAM-*b*-PDMS-*b*-PNIPAM triblock copolymer.

Michael T. Cook[*,⊥], *Sergey K. Filippov*[*,†], *Vitaliy V. Khutoryanskiy*[‖]

[†]Institute of Macromolecular Chemistry, AS CR, Heyrovsky Sq. 2, Prague, Prague 6, 162 06, Czech Republic.

[‖] School of Pharmacy, University of Reading, Whiteknights, PO Box 224, Reading, Berkshire, United Kingdom, RG6 6AD

[⊥] Department of Pharmacy & Research Centre in Topical Drug Delivery and Toxicology, University of Hertfordshire, Hatfield, Hertfordshire, United Kingdom, AL10 9AB

Abstract

In this paper, we report the synthesis and self-assembly of a novel thermoresponsive $PNIPAM_{60}$-*b*-$PDMS_{70}$-*b*-$PNIPAM_{60}$ triblock copolymer in aqueous solution. The copolymer used a commercially available precursor modified with an atom-transfer radical

polymerisation (ATRP) initiator to produce an ABA triblock copolymer via ATRP. Small-angle neutron scattering (SANS) was used to shed light on the structures of nanoparticles formed in aqueous solutions of this copolymer at two temperatures, 25 and 40 °C. The PDMS block is very hydrophobic and PNIPAM is thermoresponsive. SANS data at 25 °C indicates that the solutions of PNIPAM-*b*-PDMS-*b*-PNIPAM copolymers form well defined aggregates with presumably core-shell structure below cloud point temperature. The scattering curves originating from nanoparticles formed at 40 °C in 100% D_2O or 100% H_2O were successfully fitted with the Beaucage model describing aggregates with hierarchical structure.

1. Introduction.

Copolymers that combine blocks with different properties and different sensitivities to external stimuli in one structure attract great attention in soft matter research due to their potential biomedical applications.[1,2,3] They also have application in the field of nanoarchitectronics.[4] New chemistry approaches have been tried along with physico-chemical investigations of self-assembled structures including various types of micelles and vesicles, *etc.,* formed by such copolymers. Small-angle X-ray and neutron scattering techniques can be used to take a "closer look" at the internal structures of nanoparticles. SAXS/SANS studies have been published on a variety of block copolymers such as the diblock copolymer poly(methoxy diethylene glycol acrylate)-*block*-polystyrene (PS),[5] the diblock copolymer PS-PNIPAM[6], deuterated polystyrene and poly(n-hexyl methacrylate) (PnHMA),[7] poly(2-isopropyl-2-oxazoline)-b-poly(2-ethyl-2-oxazoline), [8] $C_{18}EO_{100}$[9], polyethylene oxide - poly(2-vinylpyridine)[10], polyethylene oxide – PNIPAM,[11,12] and PNIPAM – poly(n-butyl acrylate)[13,14] and on triblock copolymers such as (LCP, poly(4-

cyanobiphenyl-4-oxyundecylacrylate)) 'A' endblock and a deuterated polystyrene 'B' midblock,[15] PS-PMDEGA-PS,[16,17] and PS-PNIPAM-PS[18]. The most studied class of temperature-responsive polymers are poly(ethylene oxide-*block*-propylene oxide-*block*-ethylene oxide) PEO-PPO-PEO triblock copolymers known as Pluronics®.[7] Detailed SAXS/SANS studies of nanoparticle structures formed in aqueous solution have been published for a variety of commercially available Pluronics® [19] such as L44,[20] L64,[21] F127,[22,23,24] P84,[25] P85,[26,27] P104,[20] L62,[28] L64,[29] L81,[16] F68,[30] F87,[16] and F88.[16]

In our previous work, the internal structure of PNIPAM-*b*-PEG-*b*-PNIPAM nanoparticles formed in aqueous solutions was inspected by SANS upon increasing temperature.[31] Copolymers with deuterated (d-PEG) and hydrogenated central blocks (h-PEG) were synthesized to perform contrast variation experiments. Contrast variation experiments using SANS showed that the PNIPAM-*b*-PEG-*b*-PNIPAM copolymers below the cloud point existed as single polymer chains in a good solvent; a small portion of aggregates was also present in solution. In contrast, at higher temperatures, nanoparticles formed from PNIPAM-*b*-PEG-*b*-PNIPAM copolymers had a non-uniform structure with "frozen" areas interconnected by single chains in a Gaussian conformation. Such "frozen" areas were attributed to PNIPAM domains interconnected with central PEG blocks that are uniformly distributed inside of a nanoparticle.

In this article, we report a new copolymer with a central poly(dimethylsiloxane) (PDMS) block, which is considerably more hydrophobic than PEG. The substitution of hydrophobic PDMS for hydrophilic PEG may have several consequences. We can expect a significant shift of CPT to much lower values. Another shift that may be foreseen is a change in chain conformation. Unimolecular micelles or compacted macromolecular chains might occur in solution if PEG is substituted by PDMS.

The main goal of this paper was to investigate self-assembly behaviour of novel thermoresponsive triblock copolymer by dynamic light scattering and SANS and to compare this knowledge with that obtained about PNIPAM-*b*-PEG-*b*-PNIPAM in our previous study.

2. Materials and methods

2.1 Materials.

Poly(dimethylsiloxane), bis(hydroxyalkyl)-terminated (PDMS – dihydroxy) (5.2 kDa); α-bromoisobutyryl bromide (BIBB); tris(2-aminoethyl)amine (TREN); triethylamine; anhydrous tetrahydrofuran (THF); formic acid; formaldehyde; and N-isopropyl acrylamide (NIPAM) were purchased from Sigma-Aldrich (UK). Triethylamine was dried over 3 Å molecular sieves for 24 h prior to use. All other reagents were used without further purification.

2.2 Methods

2.2.1 Synthesis of the PDMS macroinitiator

PDMS – dihydroxy (1.1 mM, 3.0 mL) and triethylamine (0.15 mL) were added to a dry, sealed, round-bottom flask containing THF (5.0 mL), with stirring. The solution was degassed by nitrogen bubbling for 20 min and then cooled to 0 °C in an ice-salt bath. BIBB (1.1 mMol, 0.13 mL) was then added dropwise, and the reaction was allowed to proceed overnight. The mixture was then filtered to remove triethylamine salts and filtered. The retentate was then washed with THF (2 x 25 mL), and all THF fractions were dried *in vacuo*

to yield the PDMS macroinitiator (98% yield). ^{1}H NMR (400 MHz, $CDCl_3$, δ): 1.85 (s, CH_3), 0.00 (bs, Si-C$\underline{H}_3$) ppm.

2.2.2. Synthesis of tris[2- (dimethylamino)ethyl]amine (ME_6TREN)

ME_6TREN was synthesised using an Eschweiler-Clarke method,[32] as in a previous publication.[24] Briefly, formic acid (50 mL) was added to formaldehyde (50 mL) followed by cooling to 0 °C. TREN (4.7 mL) was subsequently added to the reaction mixture over 30 min. The reaction was then slowly brought to reflux, and the reaction was allowed to proceed for 24 h. The mixture was then concentrated under vacuum, and sodium hydroxide solution (4 M, 100 mL) was added. The product was then extracted twice into dichloromethane (75 mL) and concentrated *in vacuo* to yield a yellow liquid, ME_6TREN (3.99 g, 54% yield). ^{1}H NMR (400 MHz, $CDCl_3$, δ): 2.64 (s, 6H), 2.38 (s, 6H), 2.27 (s, 18 H) ppm. ^{13}C NMR (100 MHz, $CDCl_3$, δ): 57 ($(CH_3)_2N\underline{C}H_2$), 53 ($((CH_3)_2NCH_2\underline{C}H_2$), 46 ($CH_3$) ppm.

2.2.3. Synthesis of PNIPAM-b-PDMS-b-PNIPAM

Copper(I) chloride (0.04 mMol, 4 mg) was added to a dried round-bottom flask and sealed in. The flask was then degassed with nitrogen for 15 min. NIPAM (5.3 mMol, 600 mg), ME_6TREN (0.04 mMol, 10.7 μL), and PDMS macroinitiator (0.04 mMol, 100 mg) were added to a separate dry flask, followed by THF (5 mL). The sealed THF solution was then degassed by bubbling with nitrogen for 20 min. Using a degassed syringe, the THF solution was transferred to the flask containing copper (I) chloride. The reaction was then allowed to proceed overnight at room temperature. The product was then passed through neutral alumina to remove copper from the reaction. The resulting solution was dried *in vacuo* and then dissolved in deionised water and extensively dialysed (3.5-5 kDa MWCO membrane, Visking) against water. Yield: 55 %. ^{1}H NMR (400 MHz, $CDCl_3$, δ): 6.28 (bs, NH), 3.93 (bs,

CH PNIPAM), 3.66 (br, CH_2 PEG), 2.45-1.20 (bm, CH_2CH_2 PNIPAM), 1.07 (bs, CH_3 PNIPAM) ppm. Molecular weight of PNIPAM by NMR is 6.8 kDa (Figure S1).

The copolymer was synthesised with a central PDMS block of 5.2 kDa and terminal thermosensitive 6.8 kDa blocks of PNIPAM as determined by NMR (Figure 1, Table 1).

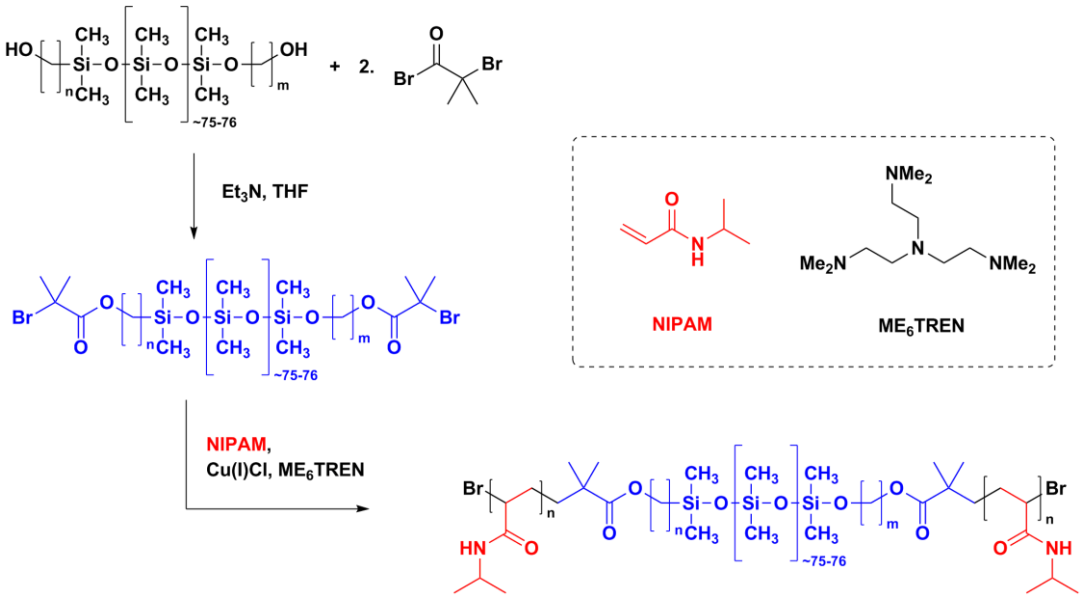

Figure 1. Synthetic route to the PNIPAM-*b*-PDMS-*b*-PNIPAM triblock copolymers

Table 1. Molecular weights of the PNIPAM-*b*-PDMS-*b*-PNIPAM triblock copolymer

Sample	Mn (kDa)	Mn of PDMS block (kDa)	Mn of PNIPAM block (kDa)	N of PNIPAM block	N of PDMS block
MTC106	18.8	5.2	6.8	60	70

2.3. Dynamic light scattering

The particle hydrodynamic radius, R_H, and scattering intensity, I_S, were measured at a scattering angle of $\theta = 173°$ using a ZetasizerNano ZS instrument, model ZEN3600 (Malvern Instruments, U.K.) with a He-Ne laser of wavelength 633 nm. Correlation functions $g^2(t)$

were analysed by a regularized inverse Laplace transformation, which provides distributions, $A(\tau)$, of relaxation times τ according to

$$g^2(t) = 1 + \beta\left[\int A(t)\exp(-t/\tau)d\tau\right]^2,$$

where β is an instrumental factor. For the diffusion of nanoparticles in liquid, the hydrodynamic radius R_H can be determined using the Stokes-Einstein equation

$$D = (\tau q^2)^{-1},$$

$$q = (4\pi n/\lambda_0)\sin(\vartheta/2)\ D = kT/6\pi\eta R_H,$$

where k is the Boltzmann constant, n the refractive index, and η the viscosity of the solvent. DLS measurements were performed for solutions of PNIPAM-*b*-PDMS-*b*-PNIPAM filtered with a 0.45 PVDF filter into a dust free cuvette. Measurements were repeated three times, and standard deviations were calculated for all measured parameters. The derived scattered intensity I_s was calculated from these experiments.

2.4. Small-angle neutron scattering (SANS)

SANS experiments were performed at instrument D11 at the Institut Laue-Langevin (ILL) in Grenoble, France. The incident neutrons had a wavelength λ = 6.0 Å with a spread of 9%. A ^{3}He gas detector with an area of 96 × 96 cm^2 and a pixel size of 7.5 × 7.5 mm^2 was used. A q-range from 0.0022 to 0.38 Å^{-1} was covered using three sample-to-detector distances: 1.2, 8, and 20 m. q is the momentum transfer, $q = 4\pi\times\sin(\theta/2)/\lambda$, with θ being the scattering angle. Samples were mounted in quartz glass cells from Hellma Analytics with a neutron path of 1 mm. At the end of each run, the sample transmission was measured. Boron carbide was used for measurement of the dark current, and H_2O was used for the detector sensitivity and calibration of the intensity. The scattered intensity curves were azimuthally averaged and corrected for background scattering from the solvent-filled cell and parasitic scattering.

Scattering from D_2O was measured separately and subtracted from the solution scattering data.

2.4.1 SANS SLD calculations

To assess the scattering of newly synthesized PNIPAM-b-PDMS-b-PNIPAM copolymer the SLD values of each block were calculated. The PDMS block has an SLD value of $0.63 \cdot 10^9$ cm^{-2}, but PNIPAM has a one-order-of-magnitude-higher SLD value of $8.1 \cdot 10^9$ cm^{-2}. We expect that in 100% D_2O, both blocks will be visible, although scattering from PNIPAM block will dominate over the scattering from PDMS block.

2.4.2 *The Beaucage fitting model*

The SANS curves in D_2O were fitted by the Beaucage model: [33,34,35]

$$I_{BC}(q) = Gexp\left(-\frac{q^2R_g^2}{3}\right) + Bexp\left(-\frac{q^2R_{sub}^2}{3}\right)\left(\frac{\left[\mathrm{erf}(qR_s/\sqrt{6})\right]^3}{q}\right)^P + G_s exp\left(-\frac{q^2R_s^2}{3}\right) + B_s\left(\frac{\left[\mathrm{erf}(qR_s/\sqrt{6})\right]^3}{q}\right)^{P_s}$$

where G is the Guinier pre-factor of the larger structure, B is a pre-factor specific to the type of power-law scattering, G_s is the Guinier pre-factor of the smaller structure, B_s is a pre-factor specific to the type of power-law scattering, R_g is the size of large-scale structure, R_{sub} is the surface-fractal cut-off radius of gyration, R_s is the size of small subunits, P is the scaling exponent of the power law assigned to the larger structure R_g, and P_s is the scaling exponent of the power law assigned to the smaller structure R_s.

3. Results and discussions

3.1 Synthesis of PNIPAM-b-PDMS-b-PNIPAM

PNIPAM-b-PDMS-b-PNIPAM was successfully synthesised by ATRP from a PDMS macroinitiator, and the structure was confirmed by NMR (Figure S1, supporting information). THF seems to be a suitable solvent for ATRP from PDMS macroinitiators, which is also suitable for many water-soluble monomers. Whilst there are a number of studies which graft PNIPAM to PDMS surfaces to modulate cell-attachment,[37,36] this is the first reported synthesis of this block copolymer, to our knowledge. Indeed, there exist few examples of any PDMS-based block copolymers synthesised by ATRP. Poly(N,N-dimethylacrylamide)-b-PDMS-b-poly(N,N-dimethylacrylamide) has been synthesised by Xu et al[38] for islet encapsulation. PDMS-b-poly(2-(dimethylamino)ethyl methacrylate) is able to form micelles to deliver chemotherapy.[39] Seo et al[40] demonstrated that poly(2-methacryloyloxyethyl phosphorylcholine)-b-PDMS-b-poly(2-methacryloyloxyethyl phosphorylcholine) was able to modify PDMS surfaces. Finally, poly(glycidyl methacrylate)-b-PDMS-b-poly(glycidyl methacrylate) has been used to create nanocomposite paper.[41]

3.2 Temperature behaviour of PNIPAM-b-PDMS-b-PNIPAM

To evaluate the temperature behaviour of PNIPAM-*b*-PDMS-*b*-PNIPAM, dynamic light scattering experiments (DLS) were conducted in aqueous solutions in H_2O. The cloud point value (CPT) was determined to be 30.0 ± 0.5 °C as the onset of a rapid increase in the derived scattered intensity I_s (Figure 2a). This CPT value is somewhat lower that the CPT for pure PNIPAM (32 °C). This discrepancy is clearly due to the presence of the hydrophobic PDMS block in the copolymer structure. The ability to reduce CPT by introducing a hydrophobic moiety has been reported previously for a variety of copolymers.[42-44] The incorporation of hydrophilic PEG as a central block creates an opposing trend – a CPT value that increases, as was previously observed for PNIPAM-*b*-PEG-*b*-PNIPAM copolymer.[27] Calculated intensity weighted distribution functions of the hydrodynamic radius R_h show a bimodal distribution at 25 °C and a monomodal distribution at 40 °C (Figure 2b, inset). The volume-weighted

hydrodynamic radius was chosen as a better representative to monitor temperature changes in comparison with the intensity-weighted R_h.

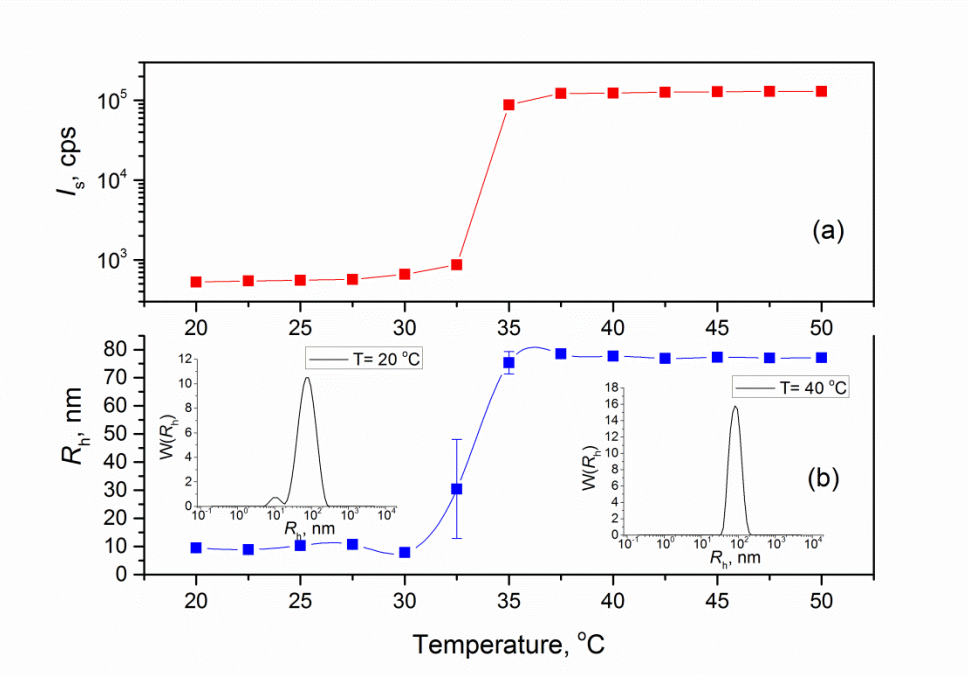

Figure 2. Temperature dependence of the scattered intensity I_s (a) and volume-weighted hydrodynamic radius (b) of the PNIPAM-*b*-PDMS-*b*-PNIPAM copolymer. Insets for the Figure 2b: intensity-weighted distribution function for hydrodynamic radius at 20 and 40 ºC.

A peculiar feature can be observed in Figure 2b. The value for R_h of 10 nm is higher than we would expect for a molecularly dissolved polymer at low temperatures below CPT. It is not surprising, however, considering the strong hydrophobicity of the PDMS block. One can expect a preliminary self-organization of copolymers even below the CPT value. Larger structures with low polydispersity indices (<0.1) were observed by DLS at elevated temperatures, as could be expected due to the thermoresponsivity of PNIPAM (Figure S2, supporting information).

SANS experiments could shed light on nanoparticle structures below and above CPT.

3.2. SANS experiments for PNIPAM-b-PDMS-b-PNIPAM

Figure 3 shows the SANS curves obtained for PNIPAM-*b*-PDMS-*b*-PNIPAM at two temperatures, 25 and 40 °C. As one can see, there is a strong variation in the SANS curves with both temperature.

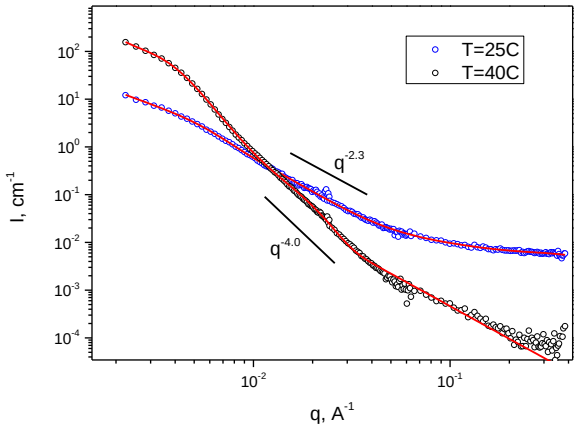

Figure 3. SANS data for the PNIPAM-*b*-PDMS-*b*-PNIPAM copolymer at two temperatures, 25 ºC and 40 ºC in D_2O. The red and blue lines are the fits by the Beaucage model.

Several features should be noted for the SANS curves at 25 and 40 °C for the PNIPAM-*b*-PDMS-*b*-PNIPAM system in D_2O (Figure 3). The curve shows $q^{-3.9}$ behaviour at 40 °C in a middle *q* range at 0.017-0.033 A^{-1}. The most spectacular modification is witnessed at middle *q* range for 25 °C. A scaling exponent value decreases to the value of -2.5. Such finding can imply that the structure of aggregates that exist in solution below CPT is different from the aggregates above CPT. The scaling exponent value close to -4 is known as Porod behaviour,[45] indicating the presence of compact objects with sharp boundaries in solution. Such findings corroborate with the DLS data described above. At a high *q* range at 0.065-0.3 A^{-1}, the scattered intensity has more gradual behaviour, with scaling exponents -1.7 and -2.3, for 25 and 40 °C, respectively. Such *q* dependence is usually attributed to macromolecular

chain conformations with excluded volume effects. The upturn at the lowest *q* visible for the SANS curve at 25 °C could be explained by the presence of fractal aggregates.

To summarize, two different types of structures were revealed by inspecting SANS curves – large objects with sharp boundaries and smaller entities with a coil conformation. To account for this complexity, the Beaucage model was applied.[33] It describes fractal aggregates consisting of smaller particles and was successfully applied for the study of a variety of soft matter systems.[46-49] From the fitting procedure, we can conclude that the sizes of whole mass fractal aggregates at 25 and 40 °C for PNIPAM-*b*-PDMS-*b*-PNIPAM are consistent with DLS data — 38 and 150 nm (Table 2). The discrepancy could be attributed to different sensitivities of the methods; DLS provides information on R_h, whereas SANS provides R_g. The subunit size R_s also depends on temperature, at 0.9 vs 8.5 nm.

Table 2. Comparison table of fitting parameters for SANS curves of PNIPAM-*b*-PDMS-*b*-PNIPAM in 100% D_2O at 25 and 40 °C.

	PNIPAM-*b*-PDMS-*b*-PNIPAM	
Fitting parameter of Beaucage model	T = 25 °C	T = 40 °C
G	5.4	5974
B	1.3± 0.3 e-5	8.29 e-10
G_s	6.2±0.3 e-3	3.76±0.01
B_s	9 ± 2 e-4	2.6 ± 0.8 e-5
R_g, nm	37.6±0.1	147.9±8.2
R_{sub}, nm	4.9±0.1	12.6±0.9
R_s, nm	0.9±0.1	8.5±0.1
P	2.7±0.1	4.0±0.1
P_s	1.6±0.2	2.28±0.01
χ^2	188	1877

In D_2O, the nanoparticle model for the PNIPAM-*b*-PDMS-*b*-PNIPAM copolymer can be described as follows: At 25 °C, a nanoparticle of overall radius of 38 nm, consisting of small 5.0 nm particles, which are arranged inside of a fractal with scaling exponent 2.7

(surface fractal). Inside the small particles, they behave as swollen macromolecular coils in good solvent; the scaling exponent is 1.6

At 40 °C, nanoparticles are much larger; R_g of 150 nm. They consist of smaller particles with 12.6 nm particles that are arranged inside of a fractal with a scaling exponent of 4.0 (surface fractal). Inside the small particles, they behave as an almost Gaussian polymer; the scaling exponent is 2.3.

CONCLUSION

Novel thermoresponsive copolymers PNIPAM-*b*-PDMS-*b*-PNIPAM were synthesised from commercially available precursors using ATRP. Using small-angle neutron scattering, we were able to investigate in detail the internal structure of nanoparticles formed from novel thermoresponsive PNIPAM-*b*-PDMS-*b*-PNIPAM triblock copolymer in aqueous solutions. In contrast with previously reported copolymers with more hydrophilic central blocks, both PNIPAM-*b*-PDMS-*b*-PNIPAM copolymers form well-defined aggregates at room temperature. The best results were obtained by application of the Beaucage model describing the nanoparticles formed at 40 °C as an aggregate with a two-level hierarchical structure.

AUTHOR INFORMATION

Corresponding Authors

Sergey K. Filippov, FAX +420-296809410, e-mail address: sfill225@gmail.com

Michael T. Cook, Tel: +44 (0)170 728 3439. e-mail: m.cook5@herts.ac.uk.

Conflict of interest

The authors declare that they have no conflict of interest.

ACKNOWLEDGEMENTS

S.F. acknowledges the Czech Science Foundation Grant No. 15-10527J. Institute Laue-Langevin is acknowledged for beam time allocation. This work was also supported by the Ministry of Education, Youth and Sports of CR within the National Sustainability Program I (Project POLYMAT LO1507). We acknowledge Isabelle Grillo, ILL, France for help with the data treatment. The work was supported within the program of Large Infrastructures for Research, Experimental Development and Innovation (Project No. LM2015050) and research project LG14037 financed by the Ministry of Education, Youth and Sports, Czech Republic.

REFERENCES

[1] Zhunuspayev DE, Mun GA, Khutoryanskiy VV (2010) Temperature-responsive properties and drug solubilization capacity of amphiphilic copolymers based on N-vinylpyrrolidone and vinyl propyl ether. Langmuir 26:7590-7597

[2] Khutoryanskaya OV, Mayeva ZA, Mun GA, Khutoryanskiy VV (2008) Designing temperature-responsive biocompatible copolymers and hydrogels based on 2-hydroxyethyl(meth)acrylates. Biomacromolecules 9:3353-3361

[3] Hruby M, Filippov SK, Panek J, Novakova M, Mackova H, Kucka J, Vetvicka D, Ulbrich K (2010) Polyoxazoline thermoresponsive micelles as radionuclide delivery systems, Macromolecular Bioscience, 10:916-924.

[4]Angelova A, Angelov B, Mutafchieva R, Lesieur S. (2015) Biocompatible Mesoporous and Soft Nanoarchitectures. Journal of Inorganic and Organometallic Polymers and Materials 25:214–32.

[4] Angelova A, Angelov B, Mutafchieva R, Lesieur S. (2015) Biocompatible Mesoporous and Soft Nanoarchitectures. Journal of Inorganic and Organometallic Polymers and Materials 25:214–32.

[5] Kyriakos K, Aravopoulou D, Augsbach L., Sapper J, Ottinger S, Psylla C, Aghebat Rafat, A, Benitez-Montoya CA, Miasnikova A, Di Z., Laschewsky A., Müller-Buschbaum P., Kyritsis A, Papadakis CM (2014) Novel thermoresponsive block copolymers having different architectures—structural, rheological, thermal, and dielectric investigations. Colloid and Polymer Science 292:1757–1774

[6] Kyriakos K., Philipp M., Lin CH., Dyakonova M., Vishnevetskaya N, Grillo I, Zaccone A, Miasnikova A, Laschewsky A, Müller-Buschbaum P, Papadakis CM (2016) Quantifying the Interactions in the Aggregation of Thermoresponsive Polymers: The Effect of Cononsolvency , Macromolecular Rapid Communications 27:420-425

[7] Ahn H, Naidu S, Ryu DY, Cho J (2009) Phase behavior of a weakly interacting polystyrene and poly(n-hexyl methacrylate) system: Evidence for the coexistence of UCST and LCST. Macromolecular Rapid Communications 30:469-474.

[8] Takahashi R, Sato T, Terao K, Qiu XP, Winnik FM (2012) Self-association of a thermosensitive poly(alkyl-2-oxazoline) block copolymer in aqueous solution. Macromolecules, 45:6111-6119.

[9] Sommer C, Pedersen JS, Garamus VM. (2005) Structure and interactions of block copolymer micelles of brij 700 studied by combining small-angle X-ray and neutron scattering. Langmuir, 21:2137-2149.

[10] Chiba A, Hashimoto T, Hasegawa H, Hadjichristidis N. (2005) Study on micro-phase separation of polyethylene oxide-poly(2-vinylpylidine) block copolymer by small-angle x-ray scattering. Polymer Preprints, 54:767.

[11]Zhao J, Zhang G, Pispas S. (2009) Morphological Transitions in Aggregates of Thermosensitive Poly(ethylene oxide)-b-poly(N-isopropylacrylamide) BlockCopolymers Prepared via RAFT Polymerization. Journal of Polymer Science: Part A: Polymer Chemistry 47:4099-4110.

[12] Papagiannopoulos A, Zhao J, Zhang G, Pispas S (2013) Thermoresponsive transition of a PEO-b-PNIPAM copolymer: From hierarchical aggregates to well defined ellipsoidal vesicles. Polymer 54:6373-6380.

[13] Škvarla J , Zedník J, Šlouf M, Pispas S, Štěpánek M (2014) Poly(N-isopropyl acrylamide)-block-poly(n-butyl acrylate) thermoresponsive amphiphilic copolymers: Synthesis, characterization and self-assembly behavior in aqueous solutions. European Polymer Journal 61:124-132.

[14] Papagiannopoulos A, Meristoudi A, Pispas S, Keiderling U (2016) Thermoresponsive behavior of micellar aggregates from end-functionalized PnBA-b-PNIPAM-COOH block copolymers and their complexes with lysozyme. Soft Matter. 12:6547-6556.

[15] Islam MT, Khan M, Shin T, Park SY. (2015) Self-assembly of a liquid crystal ABA triblock copolymer in a B-selective organic solvent. Polymer 66:94-99.

[16] Miasnikova A, Laschewsky A, De Paoli G, Papadakis CM, Müller-Buschbaum, P, Funari SS (2012) Thermoresponsive hydrogels from symmetrical triblock copolymers poly(styrene-block-(methoxy diethylene glycol acrylate)-block-styrene). Langmuir 28:4479-4490.

[17] Adelsberger J, Bivigou-Koumba AM, Miasnikova A, Busch P, Laschewsky A, Müller-Buschbaum P, Papadakis CM. (2015) Polystyrene-block-poly (methoxy diethylene glycol acrylate)-block-polystyrene triblock copolymers in aqueous solution—a SANS study of the temperature-induced switching behavior Colloid and Polymer Science 293:1515-1523.

[18] Papagiannopoulos A, Zhao J, Zhang G, Pispas S, Radulescu A. (2014) Thermoresponsive aggregation of PS-PNIPAM-PS triblock copolymer: A combined study of light scattering and small angle neutron scattering European Polymer Journal 56:59-68.

[19] Amann M, Willner L, Stellbrink J, Radulescu A, Richter D (2015) Studying the concentration dependence of the aggregation number of a micellar model system by SANS. Soft Matter 11:4208-4217.

[20] Liu Y, Chen SH. (1999) Analysis of the structure, interaction, and viscosity of pluronic micelles in aqueous solutions by combined neutron and light scatterings ACS Symposium Series 739:270-296.

[21] Lobry L, Micali N, Mallamace FC, Liao C, Chen SH. (1999) Interaction and percolation in the L64 triblock copolymer micellar system. Physical Review E - Statistical Physics, Plasmas, Fluids, and Related Interdisciplinary Topics, 60:7076-7087.

[22] Mortensen K, Talmon Y. (1995). Cryo-TEM and SANS Microstructural Study of Pluronic Polymer Solutions. Macromolecules, 28:8829–8834.

[23] Prud'homme RK, Wu G, Schneider DK. (1996) Structure and rheology studies of poly(oxyethylene-oxypropylene-oxyethylene) aqueous solution Langmuir, 12:4651-4659.

[24] Wu C, Liu T, Chu B, Schneider DK, Graziano V (1997) Characterization of the PEO-PPO-PEO triblock copolymer and its application as a separation medium in capillary electrophoresis. Macromolecules, 30:4574-4583.

[25] Liu Y, Chen SH, Huang JS (1998) Small-angle neutron scattering analysis of the structure and interaction of triblock copolymer micelles in aqueous solution. Macromolecules, 31:2236-2244.

[26] Mortensen K, Brown, WYN (1993) Poly(ethylene oxide)-Poly(propylene oxide)-Poly(ethylene oxide) Triblock Copolymers in Aqueous Solution. The Influence of Relative Block Size. Macromolecules 26:4128–4135.

[27] Mortensen K, Pedersen JS (1993) Structural study on the micelle formation of poly(ethylene oxide)-poly(propylene oxide)-poly(ethylene oxide) triblock copolymer in aqueous solution. Macromolecules, 26:805-812

[28] Hech E, Mortensen K, Hoffmann H. (1995) L3 Phase in a Binary Block Copolymer / Water System, Macromolecules. 28:5465–5476.

[29] Wu G, Chu B, Schneider DK. (1995). SANS Study of the Micellar Structure of PEO/PPO/PEO Aqueous Solution. The Journal of Physical Chemistry, 99:5094–5101.

[30] Borbély S. (1997) Small-angle neutron scattering study of Pluronic F68 tri-block copolymer solutions. Physica B: Condensed Matter, 241-243:1016-1018.

[31] Filippov SK, Bogomolova A, Kaberov L, Velychkivska N, Starovoitova L, Cernochova Z, Rogers S, Lau WM, Khutoryanskiy VV, Cook MT. (2016) Internal structure of nanoparticles formed by self-assembly of temperature-responsive PNIPAM-b-PEG-b-PNIPAM triblock copolymers: NMR and SANS studies, Langmuir, , 32:5314-5323.

[32] Opsteen JA, van Hest, J. C. M. (2007) Modular Synthesis of ABC Type Block Copolymers by ‘“ Click ”’ Chemistry. Journal of Polymer Science: Part A: Polymer Chemistry 45:2913–2924

[33] Beaucage G. (1995) Approximations leading to a unified exponential/power-law approach to small-angle scattering. Journal of Applied Crystallography.28:717–728.

[34] Hammouda B. (2010) Analysis of the Beaucage model. Journal of Applied Crystallography.43:1474–1478.

[35] Hammouda B, Jia D, Cheng D. (2015) Single-Chain Conformation for Interacting Poly(N-isopropylacrylamide) in Aqueous Solution. Journal of Science and Technology. 3:8.

[36] Ma D, Chen H, Shi D, Li Z, Wang J. (2009) Preparation and characterization of thermo-responsive PDMS surfaces grafted with poly(N-isopropylacrylamide) by benzophenone-initiated photopolymerization. Journal of Colloid and Interface Science 332:85-90.

[37] Lin JB, Isenberg BC, Shen Y, Schorsch K, Sazonova OV, Wong JY. (2012) Thermo-responsive poly(N-isopropylacrylamide) grafted onto microtextured poly(dimethylsiloxane) for aligned cell sheet engineering. Colloids and Surfaces B: Biointerfaces 1:108-15.

[38] Xu J, Qiu M, Ma B, He C. (2014) "Near Perfect" Amphiphilic Conetwork Based on End-Group Cross-Linking of Polydimethylsiloxane Triblock Copolymer via Atom Transfer Radical Polymerization. ACS Applied Materials & Interfaces 6:15283–15290

[39] Car A, Baumann P, Duskey JT, Chami M, Bruns N, Meier W. (2014) pH-Responsive PDMS-b-PDMAEMA Micelles for Intracellular Anticancer Drug Delivery. Biomacromolecules, 15:3235–3245

[40] Seo JH, Matsuno R, Konno T, Takai M, Ishihara K. (2008) Surface tethering of phosphorylcholine groups onto poly(dimethylsiloxane) through swelling deswelling methods with phospholipids moiety containing ABA-type block copolymers. Biomaterials. 29:1367-76.

[41] Song S, Zhai Y, Zhang Y. (2016) Bioinspired Graphene Oxide/Polymer Nanocomposite Paper with High Strength, Toughness, and Dielectric Constant. ACS Applied Materials & Interfaces 8:31264–31272

[42] Bogomolova A, Filippov SK, Starovoytova L, Angelov B, Konarev P, Svergun DI, Sedlacek O, Hruby M, Stepanek P (2014) Study of Thermosensitive Amphiphilic Poly-Oxazolines of Complex Nature and Their Interaction with Ionic Surfactants. Hydrophobic, Thermosensitive and Hydrophilic Moieties: Are They Equally Important? Journal of Physical Chemistry B 118: 4940-4950.

[43] Sergeeva O, Vlasov PS, Domnina NS, Bogomolova A, Konarev P, Svergun DI, Walterova Z, Horsky J, Stepanek P, Filippov SK. (2014) Novel Thermosensitive Telechelic PEGs With Antioxidant Activity: Synthesis, Molecular Properties and Conformational Behaviour. RSC Advances 4: 41763 – 41771.

[44] Filippov SK, Lezov AV, Sergeeva O, Olifirenko A, Lesnichin S, Domnina NS, Komarova E, Almgren M, Karlsson G, Štepanek P. (2008) Aggregation of dextran hydrophobically modified by sterically-hindered phenols in aqueous solutions: Aggregates vs. single molecules, European Polymer Journal. 44:3361-3369.

[45] Porod G. (1951) Die Röntgenkleinkelstreuung von Dicht Gepackten kolloiden Systemen. Kolloid-Z. 123:83-114.

[46] Stepanek M, Matejicek P, Prochazka K, Filippov SK, Angelov B, Šlouf M., Mountrichas G, Pispas S. (2011) Langmuir. 27 : 5275-5281.

[47] Papagiannopoulos A., Zhao, J., Zhang, G., Pispas, S., Radulescu, A. (2014) Thermoresponsive aggregation of PS-PNIPAM-PS triblock copolymer: A combined study of light scattering and small angle neutron scattering European Polymer Journal. 56: 59-68.

[48] Thünemann AF, Bienert R, Appelhans D, Voit B. (2012) Core-shell structures of Oligosaccharide-functionalized hyperbranched poly(ethylene imines). Macromolecular Chemistry and Physics. 213: 2362 - 2369.

[49] Izawa K., Ogasawara T., Masuda H., Okabayashi H., Monkenbusch M., O'Connor, C.J. (2002) Growth process for fractal polymer aggregates formed by perfluorooctyltriethoxysilane. Time-resolved small-angle x-ray scattering spectra and the application of the unified equation. Colloid and Polymer Science. 280: 725-735.

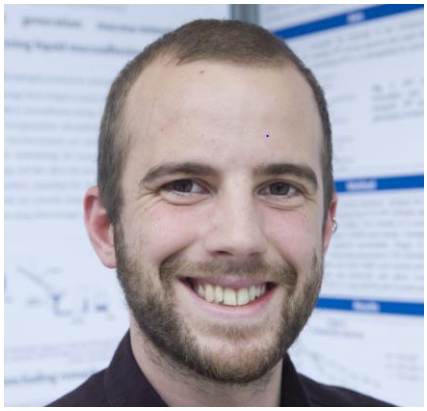

Michael Cook is a lecturer in pharmaceutics at the University of Hertfordshire, and is part of the Topical Drug Delivery and Toxicology research centre. He received his PhD from the University of Reading under the supervision of Dr Dimitris Charalampopoulos and Prof. Vitaliy Khutoryanskiy. His research is focused on the development of polymeric materials for mucosal drug delivery, with a focus on temperature-responsive materials. He is also interested in the use of hydrogels as biomimetic materials.

Sergey Filippov received a B.S., M.Sc. with honors and Ph.D. in polymer physics from the University of Saint-Petersburg, Russia. His Ph.D. thesis was devoted to polymeric liquid crystals. During his Ph.D. studies he spent one year in Oxford University in the group of Prof. Steve Elston. Between 1999 and 2001, he was employed as a postdoctoral researcher at Puerto Rico University where he used dynamic light scattering and broadband dielectric spectroscopy to study polymers and confined liquid crystals. In 2002 he re-joined the Saint-Petersburg State University as an assistant professor. His major field of expertise was dynamic light scattering in polymer solutions. In 2007 he joined the Institute of Macromolecular Chemistry in Prague, Czech Republic as a research scientist on the of Department of Supramolecular Polymer Systems, headed by Petr Štěpánek. In 2014, he became a senior research scientist on the same Department. Dr. Filippov's main research interests are dynamic light scattering, small-angle X-ray and neutron scattering, and isothermal titration calorimetry in application to self-assembling systems in soft matter.

Vitaliy Khutoryanskiy is Professor of Formulation Science (since August 2014), having previously been Associate Professor (Reader) in Pharmaceutical Materials (2010-2014) and Lecturer in Pharmaceutics (2005-2010) at Reading School of Pharmacy, University of Reading, UK. Prior to Reading, he worked as a Research Associate in the School of Pharmacy and Pharmaceutical Sciences, University of Manchester, UK (2004-2005), as Research Fellow in the Department of Pharmaceutical Sciences, University of Strathclyde, UK (2002-2005) and as a Lecturer in Polymer Chemistry, Kazakh National University, Kazakhstan (2000-2002). He received his PhD in Polymer Chemistry in 2000 from Kazakh National Technical University, Kazakhstan. Prof Khutoryanskiy has researched broadly in the area of materials for pharmaceutical and biomedical applications, with a particular emphasis on drug delivery, mucoadhesive materials, hydrogels, and stimuli-responsive polymers. He was the recipient of the 2012 McBain Medal (Society of Chemical Industry and Royal Society of Chemistry (RSC)) for his imaginative use of colloid, polymer and interface science in the development of novel biomedical materials. He has published over 120 original research articles, 14 reviews in peer reviewed journals, and edited 2 books.